PHOTOSYNTHETICA
International Journal for Photosynthesis Research

DOI 10.32615/ps.2022.039 PHOTOSYNTHETICA 61 (SI): 177-189, 2023

Special issue on Recent advances in photomodulation in higher plants, algae, and bryophytes

Moderate photoinhibition of PSII and oxidation of P700 contribute to chilling tolerance of tropical tree species in subtropics of China

V.S.J. SUNOJ[*,+], Y. WEN[*], A. JAJOO[**], A.W. SHORT[*,***], W.H. ZENG[*], N.I. ELSHEERY[#], and K.F. CAO[*,+]

State Key Laboratory for Conservation and Utilization of Subtropical Agri-Bioresources and Guangxi Key Laboratory of Forest Ecology and Conservation, College of Forestry, Guangxi University, 530004 Nanning, Guangxi, China[*]
School of Life Science, Devi Ahilya University, 452017 Indore, India[**]
Department of Agricultural Botany, Tanta University, 72513 Tanta, Egypt[#]
Institute of Ecology and Evolution, University of Oregon, Eugene, OR 97403, USA[***]

Abstract

In the subtropics, a few tropical tree species are distributed and planted for ornamental and horticultural purposes; however, the photosynthesis of these species can be impaired by chilling. This study aimed to understand how these species respond to chilling. Light-dependent and CO_2 assimilation reactions of six tropical tree species from geographically diverse areas, but grown at a lower subtropical site in China, were monitored during a chilling (≤ 10°C). Chilling induced stomatal and nonstomatal effects and moderate photoinhibition of PSII, with severe effect in *Ixora chinensis*. *Woodfordia fruticosa* was little affected by chilling, with negligible reduction of photosynthesis and PSII activity, higher cyclic electron flow (CEF), and oxidation state of P700 ($P700^+$). Photoinhibition of PSII thus reduced electron flow to P700, while active CEF reduced oxidative damage of PSI and maintained photosynthesis during chilling. Studied parameters revealed that coupling between light-dependent and CO_2 assimilation reactions was enhanced under chilling.

Keywords: chilling; cyclic electron flow; oxidation of P700; photoinhibition; photosynthesis.

Highlights

- Chilling induced stomatal and nonstomatal effects and moderate photoinhibition of PSII
- Photoinhibition of PSII, photosynthesis control, and CEF sustained oxidation of P700
- Oxidation of P700 reduced oxidative damage and maintained photosynthesis during chilling

Received 19 May 2022
Accepted 9 August 2022
Published online 15 September 2022

[+]Corresponding author
e-mail: johnsunoj.valiaparam@ag.tamu.edu
kunfangcao@gxu.edu.cn

Abbreviations: CE – carboxylation efficiency; CEF – cyclic electron flow; C_i – internal CO_2 concentration; $ETR_{(I)}$ – photosynthetic electron flow through PSI; $ETR_{(II)}$ – photosynthetic electron flow through PSII; Fd – ferredoxin; F_v/F_m – maximum quantum yield of PSII in the dark-adapted state; g_s – stomatal conductance; LEF – linear electron flow; NPQ – nonphotochemical quenching; P680 – chlorophyll *a* of PSII reaction centers; $P680^+$ – oxidized P680; P680* – excited P680; P700 – chlorophyll *a* of PSI reaction centers; $P700^+$ – oxidized P700; P700* – excited P700; PC – plastocyanin; P_m – maximum photooxidizable P700; P_N – net photosynthetic rate; PQ – plastoquinone; RISE – reduction-induced suppression of electron flow; $Y_{(I)}$ – effective photochemical quantum yield of PSI; $Y_{(II)}$ – effective photochemical quantum yield of PSII; $Y_{(CEF)}$ – effective quantum yield of CEF; $Y_{(NA)}$ – acceptor-side limitation of PSI; $Y_{(ND)}$ – donor-side limitation of PSI; $Y_{(NO)}$ – yield of regulated heat dissipation of PSII; $Y_{(NPQ)}$ – effective quantum yield of NPQ or regulated nonphotochemical quenching; ΔpH – proton gradient.

Acknowledgments: We thank Hans Lambers of the University of Western Australia, Australia for critical comments, corrections, and editing and Junjie Zhu of Guangxi University, China for the technical advice on *Dual PAM-100* operations. This work was supported by the National Natural Science Foundation of China (31861133008, 31470469), and by the postdoctoral fellowship from Guangxi University, China, granted to John Sunoj Valiaparambil Sebastian, and the Bagui Scholarship (C33600992001) granted to Kun-fang Cao.

Conflict of interest: The authors declare that they have no conflict of interest.

Introduction

Tropical plants grow in hot and humid climatic conditions with minor seasonal temperature variations. However, the chilling tolerance of some tropical plant species enables them to survive in marginal tropical and lower subtropical areas (subtropics with relatively low latitudes), where short-term chilling events (≤ 10°C for a few days) frequently occur during winter. A few selected tropical tree species have been planted in marginal tropical and lower subtropical areas for ornamental and horticultural purposes (Jalili *et al.* 2010, Li *et al.* 2016, Mau *et al.* 2018). Chilling during winter in the lower subtropics is a major factor limiting the latitudinal distribution and poleward migration of tropical plant species, despite global warming (Li *et al.* 2016, Wen *et al.* 2018). Chilling stress is complex and adversely affects the morphological, physio-biochemical, and molecular processes in plants, thus it reduces their growth and development (Allen and Ort 2001, Liu *et al.* 2018, Elsheery *et al.* 2020, Li *et al.* 2021, Mathur *et al.* 2021). Earlier studies have revealed the influence of chilling in combination with varying incident light intensities on photosynthesis and photoprotection mechanisms of plants, including diverse tropical tree species (Someralo and Krause 1990, Barth and Krause 1999, Elsheery *et al.* 2008, Huang *et al.* 2010a,b; 2011, 2017; Zheng *et al*. 2016, Yang *et al.* 2017).

During photosynthesis, the antenna complexes of PSII and PSI absorb light energy and drive the electron flow to generate energy-rich compounds (ATP and NADPH), which are utilized to fix CO_2, converting it into carbohydrates (Miyake 2020). Under chilling, due to stomatal and nonstomatal control of CO_2 fixation, Chl *a* of reaction centers of the photosystems (P700 in PSI [excited; P700*] and P680 in PSII [excited; P680*]) cannot be de-excited to their ground state (Allen and Ort 2001). The failure of de-excitation of reaction centers of photosystems alters the photosynthetic electron transport. Such circumstances result in a reduction of O_2 (Mehler reaction) and produce reactive oxygen species (ROS) such as superoxide ($O_2^{\bullet-}$) and hydrogen peroxide (H_2O_2). The production of ROS contributes to the generation of hydroxyl radicals ($^{\bullet}OH$), which can damage DNA, proteins, and lipids. In contrast, the oxidized reaction centers of chlorophyll P680 in PSII ($P680^+$) are reduced by accepting electrons, resulting from the oxidation of water and forming singlet P680 ($^1P680^*$). Failure to de-excite $^1P680^*$ leads to the production of triplet chlorophyll ($^3P680^*$), which can transfer the energy to ground state oxygen ($^3O_2$), resulting in the production of singlet oxygen ($^1O_2$), a harmful ROS similar to $O_2^{\bullet-}$. High concentrations of ROS trigger a higher level of photoinhibition or inactivation of photosystems which is detrimental to plant survival under chilling (Allen and Ort 2001, Müller *et al*. 2001, Rutherford and Krieger-Liszkay 2001, Miyake 2010, 2020). However, among photosystems, PSII is more sensitive to chilling than PSI in a range of tropical tree species (Someralo and Krause 1990, Barth and Krause 1999, Huang *et al*. 2010a,b).

Photoinhibition of PSI occurs when PSII transfers electrons beyond the electron-accepting capacity of PSI. Compared with PSII, the PSI reaction centers require more time to recover from ROS-mediated oxidative damage (Zhang *et al.* 2004, Zivcak *et al.* 2015), which can be lethal due to the inefficiency of plants to cope with extensive loss/inhibition of PSI (Sonoike 1996, 2011; Guidi *et al*. 2019). Therefore, protection of PSI from oxidative damage by keeping P700 in an oxidized state ($P700^+$) is crucial to the survival of plants under chilling (Kubo *et al.* 2011, Sonoike 2011). Photoinhibition of PSII and subsequent reduction of electron flow to PSI in tropical trees under chilling protects PSI from chilling injury by supporting a sustainable $P700^+$ state (Huang *et al.* 2010a, Sonoike 2011, Miyake 2020). Hence, moderate photoinhibition of PSII throughout unfavorable conditions is considered a first-level photoprotection mechanism (Murchie and Niyogi 2011, Tikkanen *et al.* 2014). However, higher, and prolonged photoinhibition of PSII and PSI leads to the accumulation of ROS, which damages DNA, proteins, and lipids. Damage to the lipids of the thylakoid membrane increase membrane fluidity, resulting in the destruction of the photosynthetic apparatus and thus the impairment of photosynthesis and growth (Derks *et al.* 2015, Elsheery *et al*. 2020).

Irrespective of the photosystems, the change in the magnitude of photoinhibition from moderate to severe is a consequence of the intensity and duration of chilling, the high intensity of incident light during the stress period, lower CO_2 fixation, and linear electron flow (LEF) between PSII to PSI and the failed de-excitation of photosystem reaction centers (P700* and P680*) to an oxidized state ($P700^+$ and $P680^+$). In other words, the extent of photoinhibition is intensified by a combination of the longer duration of excitation status of P700 and P680, high content of ROS, inability to avoid oxidative damage by activation of various photoprotection mechanisms, nonenzymatic scavenging of ROS, and delayed recovery from chilling injuries (Asada 2006, Khatoon *et al.* 2009, Murata *et al.* 2007, 2012; Miyake 2010, 2020; Huang *et al.* 2011).

ROS are strong signaling molecules involved in plant growth and development as well as primary signals for stress responses; their excess production and high content can have a negative impact on plant development (Foyer and Shigeoka 2011, Zheng *et al.* 2019). Effective regulation of the excess energy in photosystems before the surplus production of ROS, and timely removal of ROS, relies on photoprotection mechanisms such as (*1*) cyclic electron flow (CEF) around PSI, (*2*) nonphotochemical quenching (NPQ) to dissipate excess absorbed light energy, (*3*) water–water cycle (WWC) or the Mehler–ascorbate peroxidase pathway (MAP) (Miyake 2010, Neto *et al.* 2017), and (*4*) photorespiration (Asada 2006). Hence, CEF, NPQ, and WWC under stress conditions are vital for stress tolerance and the subsequent recovery from stress. The activation of the above-mentioned photoprotective mechanisms under chilling is entirely dependent on the magnitude of the chilling tolerance of a plant, and the efficiency of such

mechanisms determines the chilling tolerance of a plant. Other important mechanisms, such as regulation of the stomatal opening and closing (stomatal behavior) (Raven 2014, Jurczyk *et al.* 2019) and reducing side heterogeneity of PSII, antenna size heterogeneity of PSII (Bukhov and Carpentier 2000, Belgio *et al*. 2014, Mathur *et al.* 2021), and anatomical and morphological alterations (Gratani *et al.* 2013, Wu *et al.* 2022), are equally crucial for chilling tolerance. The chilling tolerance of plant species can be genetic, which is permanent within the lifespan of a plant species, and phenotypic, which is reversible according to the existing microclimatic conditions, called evolutionary adaptation and acclimation or morphophysiological adjustments, respectively (Körner 2016).

A few studies have been conducted to understand the photoprotection mechanisms and sensitivity of photosystems in tropical tree species found in the marginal tropics of China (Huang *et al.* 2010a,b; 2011, 2017; Zheng *et al.* 2016, Yang *et al.* 2017). However, such studies were conducted at the seedling stage with artificial chilling treatments for a short duration (hours), and their results demonstrate the activation of photoprotection mechanisms, *i.e*., CEF and NPQ. Furthermore, these studies have also demonstrated reduced maximum photochemical efficiency of PSII (F_v/F_m), the effective photochemical quantum yield of PSII [$Y_{(II)}$] and PSI [$Y_{(I)}$], nonphotochemical quenching (NPQ), PSI acceptor-side limitation [$Y_{(NA)}$] and foliar gas exchange along with higher PSI donor-side limitation [$Y_{(ND)}$] and quantum yield of nonregulated energy dissipation [$Y_{(NO)}$] in response to chilling. At the same time, maximum photooxidizable P700 (P_m) was higher or stable in tropical trees under chilling. In this study, we sought to provide photosynthetic responses of geographically diverse tropical tree species to a realistic seasonal chilling event under the prevailing ambient microclimatic conditions in open fields of a lower subtropical site in China during winter, rather than using seedlings and artificial induction of chilling. Our primary target was to grade the tested tropical plant species in a lower subtropical site in China according to the magnitude of their chilling tolerance and compare and validate the physiological response of the current study with the earlier studies. The specific objectives of this study were to address the following questions: (*1*) How is the magnitude of chilling tolerance of tropical tree species in the lower subtropics related to the physiological mechanisms involved in photosynthesis? And (*2*) how are light-dependent and CO_2 assimilation reactions coupled to each other in tested tropical trees under a chilling event during winter as compared with summer? We tested the hypothesis that, under chilling, maintaining the $P700^+$ state in PSI and related suppression of oxidative damage retains limited photosynthesis, and the tight coupling of light-dependent and CO_2 assimilation reactions support the chilling survival of tropical trees in the lower subtropics.

Materials and methods

Plant materials and growth conditions: The present study was conducted in January 2018 (winter; average day/night temperature: 13/11°C) and July 2018 (summer; average day/night temperature: 28/25°C) on the campus of Guangxi University, Nanning, China (22.83°N, 108.28°E). For this experiment, adult plants of six tropical tree species grown in an open field were selected based on geographical diversity (*see* text table below).

Physiological traits were recorded for fully mature leaves, which were exposed to sunlight during winter and summer. Before the physiological traits were recorded the experimental site received 11.7 mm of rainfall from 4 to 7 January 2018 and 78.9 mm from 1 to 15 July 2018 (Fig. 1S, *supplement*). Therefore, the soil was wet during the measurements in both seasons. A temperature drop to ≤ 10/≤ 6°C in day/night for four days during winter was considered a chilling event.

Photosynthetic rate, stomatal conductance, and carboxylation efficiency: In both seasons (winter and summer), photosynthetic rate (P_N), stomatal conductance (g_s), and internal CO_2 concentration (C_i) of six tree species were recorded using a portable photosynthesis system (*LI-6800*, *LICOR*, Lincoln, NE, USA). From each species, a minimum of nine measurements were recorded between 9:00 to 11:00 h from three individual plants. The leaf was illuminated by PAR of 1,000 µmol(photon) m^{-2} s^{-1} provided by a red-blue light-emitting diode (LED), whereas ambient CO_2, temperature, and relative humidity (RH) were used during the measurement of gas exchange. Carboxylation efficiency (CE) was calculated from the ratio of P_N to C_i (Rymbai *et al.* 2014).

Chlorophyll (Chl *a*) fluorescence and P700 measurements: Chl fluorescence and P700 measurements were

Botanical name	Family	Geographic distribution
Ixora chinensis Lam.	Rubiaceae	Southern China and southeastern Asia
Aglaia odorata Lour.	Meliaceae	Native to Taiwan and subtropical mountain regions of southern China
Lagerstroemia speciosa L.	Lythraceae	Tropical southern Asia
Dypsis lutescens (H. Wendl.)	Arecaceae	Madagascar, Andaman Islands, Reunion, El Salvador, Cuba, Puerto Rico, the Canary Islands, southern Florida, Haiti, the Dominican Republic, Jamaica, the Leeward Islands, and the Venezuelan Antilles
Markhamia stipulata (Wall.)	Bignoniaceae	South China to Southeast Asia
Woodfordia fruticosa L.	Lythraceae	Tanzania, Madagascar, Comores, Saudi Arabia, Oman, Myanmar (Burma), Bhutan, Indonesia, China, India, Sri Lanka, Nepal, Pakistan, and Vietnam

performed in both seasons using a *Dual PAM-100* (*Heinz Walz*, Effeltrich, Germany). The transients were recorded at 25°C from the leaves of six detached branches of three individual trees. Immediately after detaching branches from the trees, basal parts of branches were immersed in distilled water and transported to the laboratory. First, dark-adapted F_0 and F_m were determined in fully exposed mature leaves after 30 min of dark adaptation and by applying a saturation pulse of 10,000 µmol(photon) m^{-2} s^{-1} for 300 ms. Photochemical efficiency of PSII (F_v/F_m) was calculated as $F_v/F_m = (F_m - F_0)/F_m$; where F_0 is the minimum fluorescence and F_m the maximum in the dark-adapted state.

After determining F_0 and F_m, light-adapted Chl fluorescence transients and P700 measurements were measured. The mode of collection of branches, number of replications, and recording temperature was the same as for dark-adapted measurements. Before the light-adapted measurements, leaves were light-adapted for 30 min under PAR of 500 µmol(photon) m^{-2} s^{-1}; and then Chl fluorescence and P700 transients were recorded after 3 min exposure to light intensity of 10,000 µmol(photon) m^{-2} s^{-1} by placing the leaf between the measuring head of the *Dual PAM-100*. The light-adapted Chl fluorescence transients were calculated as $Y_{(II)} = (F_m' - F_s)/F_m'$, $Y_{(NO)} = F_s/F_m'$, and $Y_{(NPQ)} = 1 - Y_{(II)} - Y_{(NO)}$ (Genty *et al.* 1989, Oxborough and Baker 1997, Kramer *et al.* 2004); where $Y_{(II)}$ is the effective photochemical quantum yield of PSII, $Y_{(NO)}$ is the quantum yield of nonregulated energy dissipation, $Y_{(NPQ)}$ is the fraction of energy dissipated as heat through regulated nonphotochemical quenching (NPQ), F_m' is light-adapted state maximum fluorescence, and F_s is light-adapted state steady-state fluorescence (Kramer *et al.* 2004).

The maximum photooxidizable P700 in PSI (P_m) was determined by applying far-red light for 10 s, followed by a saturation pulse of 10,000 µmol(photon) m^{-2} s^{-1} for 300 ms after 30 min of dark adaptation. The P_m represents the maximum change of the P700 signal from fully reduced state P700 (minimum signal; P700) to the fully oxidized state P700 (maximum; $P700^+$) upon application of a saturation pulse. P_m allows the scaling of the P700 signal and is an essential prerequisite for the determination of P700 transients, similar to F_m of chlorophyll fluorescence transient. Other PSI transients were calculated from the light-adapted transients and predetermined $P700^+$ as follows: $Y_{(I)} = 1 - Y_{(ND)} - Y_{(NA)}$; where $Y_{(ND)} = 1 - P700(red)$ [$Y_{(ND)} = 1 - Y_{(I)}$], $Y_{(NA)} = (P_m - P_m')/P_m$; $Y_{(I)}$ is the effective photochemical quantum yield of PSI, which is defined by the fraction of overall P700 reduced in a given state and not limited by the acceptor side [$Y_{(NA)}$]. Donor-side limitation [$Y_{(ND)}$] is the fraction of overall P700 oxidized in a given state and $Y_{(NA)}$ (acceptor-side limitation) represents the fraction of P700 that cannot be oxidized by a saturation pulse in a given state due to a lack of acceptors; $Y_{(NA)}$ reflects the inability of far-red light to oxidize all P700. At the same time, maximum photooxidizable P700 in a given light state (P_m') upon application of the saturation pulse is similar to F_m' of Chl fluorescence at light-adapted state. P700(red), which was determined in a given state with the help of the saturation pulse, represents the fraction of overall P700 reduced for a given state (Klughammer and Schreiber 1994, 2008).

Estimation of LEF and CEF: Linear electron flow from PSII to PSI (LEF [µmol(e^-) m^{-2} s^{-1}]; electron transport rate of PSII [$ETR_{(II)}$] [µmol(e^-) m^{-2} s^{-1}] and electron transport rate of PSI [$ETR_{(I)}$] [µmol(e^-) m^{-2} s^{-1}], respectively) in the six selected species were calculated using the following formula: $ETR_{(II)} = Y_{(II)} \times ab\ I \times PAR \times 0.5$ and $ETR_{(I)} = Y_{(I)} \times ab\ I \times PAR \times 0.5$; where, ab I (0.84) is the light absorptance ratio of a leaf and 0.5 is a theoretical factor based on the assumption that reaction centers of the chlorophylls in both photosystems absorb 50% of incident light (Maxwell and Johnson 2000). The value of CEF was estimated as: $CEF = ETR_{(I)} - ETR_{(II)}$ [data not shown in the manuscript as $Y_{(CEF)}$ is representative of CEF], and $Y_{(CEF)}$ was estimated as: $Y_{(CEF)} = Y_{(I)} - Y_{(II)}$ (Miyake *et al.* 2005a,b).

The outputs from the *Dual PAM-100* may somewhat underestimate LEF; consequently, they overestimate CEF as the *Dual PAM-100* measures Chl *a* fluorescence from leaf mesophyll cells near the leaf surface while P700 comprises the signal from the whole leaf (Huang *et al.* 2011). Despite this inaccuracy, earlier researchers and we believe that relative changes in LEF and CEF in response to chilling are reliable to understand the relative seasonal changes (Miyake *et al.* 2005a,b; Huang *et al.* 2010a,b; 2011, 2015; Gao and Wang 2012).

Statistical analysis: Correlation analysis between actual ambient light-independent reaction values and potential light-dependent reaction values of both seasons was executed using *Sigma Plot* (*ver. 10*, *Systat Inc.*, USA). For statistical analysis of the data, three biological replications per species were used for each collected parameter and season. We used analysis of variance (*ANOVA*) to test for significant differences in all measured physiological parameters among species and between seasons. Generalized linear models (GLM) in *SPSS* (*ver. 10*, *SPSS Inc.*, USA) were used to assess the effects of species and season on the measured physiological parameters. For the statistical comparison between the two seasons for each species, a *Student*'s *t*-test was conducted.

Results

We observed significant differences in various physiological parameters and responses of the studied tree species between seasons (Table 1). F_v/F_m was significantly reduced under chilling in all species, except for *Woodfordia fruticosa*, which displayed no change in F_v/F_m and the smallest reduction in photosynthesis compared to the other species (Fig. 1). Among the six species, three species had F_v/F_m values of 0.6–0.7 during the chilling period; *Ixora chinensis* had an F_v/F_m value of 0.43, and *W. fruticosa* maintained an F_v/F_m value above 0.78 during both seasons. $Y_{(NPQ)}$ was reduced in all species studied and the smallest reduction was observed in *Aglaia odorata* and *W. fruticosa*

Table 1. Effect of chilling event on light-energy utilization in PSII, redox state of PSI, and cyclic electron flow (CEF) in comparison with those in summer. The values in parentheses indicate the percentage change in winter compared with summer. Statistical comparison between both seasons for individual species indicated by * and ** corresponding to significance at $P<0.05$ and $P<0.01$, respectively. NS indicates nonsignificant. $ETR_{(I)}$ – photosynthetic electron flow through PSI; $ETR_{(II)}$ – photosynthetic electron flow through PSII; LEF – linear electron flow; P_m – maximum photooxidizable P700; $Y_{(I)}$ – effective photochemical quantum yield of PSI; $Y_{(II)}$ – effective photochemical quantum yield of PSII; $Y_{(CEF)}$ – effective quantum yield of CEF; $Y_{(NA)}$ – acceptor-side limitation of PSI; $Y_{(ND)}$ – donor-side limitation of PSI; $Y_{(NO)}$ – yield of regulated heat dissipation of PSII; $Y_{(NPQ)}$ – effective quantum yield of NPQ or regulated nonphotochemical quenching.

	Ixora chinensis		*Aglaia odorata*		*Lagerstroemia speciosa*		*Dypsis lutescens*		*Markhamia stipulata*		*Woodfordia fruticosa*	
	Winter	Summer	Winter	Summer	Winter	Summer	Winter	Summer	Winter	Summer	Winter	Summer
$Y_{(II)}$	0.03 (–57%)*	0.07	0.04 (–33%)*	0.06	0.09 (–19%)*	0.11	0.05 (–29%)*	0.07	0.06 (–14%)*	0.07	0.22 (+57%)*	0.14
$Y_{(I)}$	0.07 (–50%)*	0.14	0.08 (–38%)*	0.13	0.16 (–6%)NS	0.17	0.08 (–38%)*	0.13	0.09 (–36%)*	0.14	0.35 (+67%)*	0.21
$Y_{(NPQ)}$	0.23 (–68%)*	0.71	0.32 (–55%)*	0.71	0.12 (–83%)**	0.69	0.17 (–75%)**	0.68	0.14 (–81%)**	0.73	0.28 (–57)*	0.65
$Y_{(NO)}$	0.74 (+236%)**	0.22	0.64 (+178%)**	0.23	0.81 (+268%)**	0.22	0.78 (+212%)**	0.25	0.80 (+321%)**	0.19	0.50 (+138%)**	0.21
P_m	2.4 (+322%)**	0.6	1.8 (+239%)**	0.5	2.7 (+435%)**	0.5	1.3 (+306%)**	0.3	2.0 (+115%)**	0.9	2.5 (+462%)**	0.4
$Y_{(CEF)}$	0.04 (–33%)*	0.06	0.04 (–43%)*	0.07	0.08 (+1%)NS	0.08	0.05 (–7%)*	0.06	0.03 (–57%)*	0.07	0.13 (+86%)*	0.07
$Y_{(ND)}$	0.85 (+21%)*	0.70	0.85 (+35%)*	0.63	0.71 (+13%)*	0.63	0.84 (+14%)*	0.74	0.85 (+29%)*	0.66	0.55 (+15%)*	0.48
$Y_{(NA)}$	0.08 (–53%)*	0.17	0.07 (–71%)**	0.24	0.14 (–26%)*	0.19	0.09 (–31%)*	0.13	0.06 (–70%)**	0.20	0.11 (–65%)*	0.31
LEF [$\mu mol(e^-)\ m^{-2}\ s^{-1}$]	37.9 (–53%)*	80.4	47.5 (–36%)*	74.1	106.0 (+2%)NS	104.0	50.3 (–35%)**	77.8	59.0 (–29%)*	83.0	127.0 (–7%)*	136.0
$ETR_{(I)}$ [$\mu mol(e^-)\ m^{-2}\ s^{-1}$]	26.0 (–50%)*	52.5	31.8 (–36%)*	49.9	65.4 (–3%)NS	67.6	34.1 (–33%)*	51.0	35.5 (–35%)*	54.7	77.5 (–5%)*	81.8
$ETR_{(II)}$ [$\mu mol(e^-)\ m^{-2}\ s^{-1}$]	11.9 (–57%)*	27.9	15.7 (–35%)*	24.1	40.1 (+12%)*	35.9	16.2 (–40%)*	26.8	23.5 (–17%)*	28.3	49.7 (–10%)*	54.1

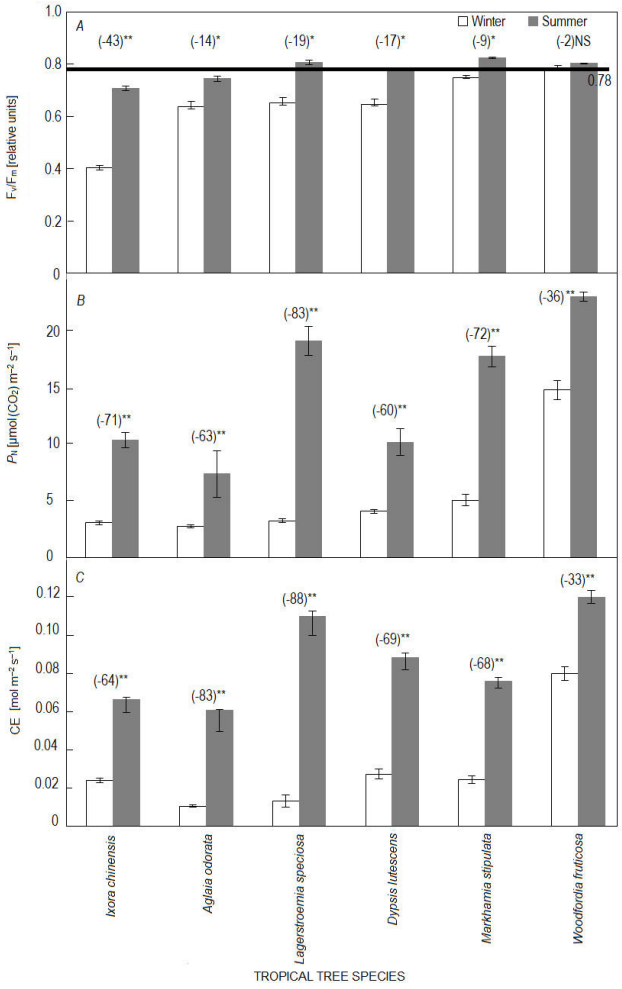

Fig. 1. Differences in (*A*) maximum photochemical efficiency of PSII (F_v/F_m), (*B*) net photosynthetic rate (P_N), and (*C*) carboxylation efficiency (CE) during the chilling event (≤ 10°C; *white bars*) and summer (≥ 27°C; *gray bars*) among six tropical tree species. *The white and gray bars* indicate the means and standard errors. The values in the parentheses indicate a relative change in the winter values compared with the summer. *The black line* across Fig. 1*A* indicates F_v/F_m value of 0.78. Statistical comparison between both seasons for individual species indicated by NS, *, and ** corresponding to non-significance, significance at $P<0.05$ and $P<0.01$, respectively.

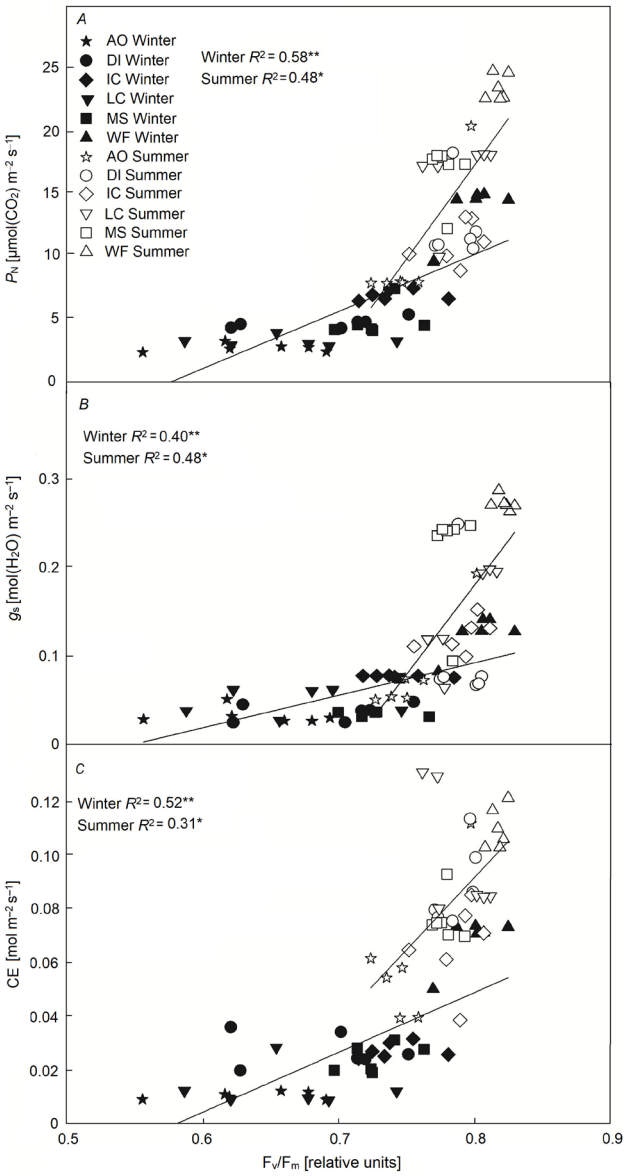

Fig. 2. Correlation of maximum quantum yield of PSII in the dark-adapted state (F_v/F_m) with (*A*) net photosynthetic rate (P_N), (*B*) stomatal conductance (g_s), and (*C*) carboxylation efficiency (CE) during the chilling event (≤ 10°C; *closed symbols*) and summer (≥ 27°C; *open symbols*) among six tropical tree species. Coefficient of determination (R^2) followed by * and ** corresponding to significance at $P<0.05$ and $P<0.01$, respectively. AO – *Aglaia odorata*; DI – *Dypsis lutescens*; IC – *Ixora chinensis*; LS – *Lagerstroemia speciosa*; MS – *Markhamia stipulata*; WF – *Woodfordia fruticosa*.

(Table 1). In contrast, P_m was 15 to 462% higher across species under chilling compared to measurements made in summer (Table 1). CEF under chilling was the highest in *W. fruticosa* followed by *Lagerstroemia speciosa*, and lower in *Markhamia stipulata*, *A. odorata*, and *I. chinensis*.

Effect of chilling event on gas exchange and their relationship with F_v/F_m: Besides the significant reduction of F_v/F_m in five of the species (Fig. 1), P_N, g_s, and CE were significantly reduced in all species under chilling, and positively correlated with F_v/F_m across species during each season, respectively (Fig. 2). *Lagerstroemia speciosa* showed the greatest reduction in P_N and CE, while *W. fruticosa* showed higher P_N and CE than any other species in both seasons, with the lowest reduction under chilling; and the lowest P_N and CE was in *A. odorata* (Fig. 1).

Effect of chilling event on light-energy utilization by PSII, redox state of PSI, and CEF: We observed lower values of $Y_{(II)}$ and $Y_{(I)}$ under chilling across species, except for *W. fruticosa*, which had higher values than any of the other species for the above parameters (Table 1; Fig. 2S, *supplement*). Concomitantly, $Y_{(NPQ)}$ was reduced across all species, whereas $Y_{(NO)}$ increased. The difference in $Y_{(NO)}$ and CEF among species was minimal during summer compared with the difference under chilling. A faster rate of photosynthetic electron flow through PSII and PSI [LEF; $ETR_{(II)}$ and $ETR_{(I)}$] was recorded in *W. fruticosa* during both seasons among all species studied. In contrast, LEF was low in *I. chinensis* under chilling. Furthermore, we measured a higher CEF during summer compared to chilling in all species except for *W. fruticosa* and *L. speciosa*. Finally, $Y_{(ND)}$ and P_m increased, whereas $Y_{(NA)}$ decreased in all species under chilling. In contrast, $Y_{(ND)}$ and P_m were lower in *W. fruticosa* (Table 1).

Relationship of light energy utilization in PSII with the redox state of PSI and CEF: We detected negative correlations between $Y_{(ND)}$ and $Y_{(II)}$ and $Y_{(ND)}$ and LEF across species in each season; however, the correlation was stronger during winter. Furthermore, the negative correlation between $Y_{(ND)}$ and CEF across species was only observed during winter (Fig. 3). In contrast, there were no correlations between $Y_{(NA)}$ and the above parameters in either season, whereas CEF showed significant positive correlations with LEF and $Y_{(II)}$ only during winter (Fig. 4). We observed negative correlations between $Y_{(NO)}$ and $Y_{(NPQ)}$ (Fig. 5*A*), and between $Y_{(NA)}$ and $Y_{(ND)}$ (Fig. 5*C*) across species in each season, whereas $Y_{(I)}$ and $Y_{(II)}$ were significantly and positively correlated across species in each season (Fig. 5*B*).

Discussion

Chilling affects many components related to photosynthesis (Allen *et al.* 2000, Allen and Ort 2001), including nonstomatal regulation, *i.e.*, electron transport between photosystems in thylakoid membrane and activities of CO_2 assimilation reactions of photosynthesis, photorespiration, and stomatal functioning. Both CO_2 fixation and PSII and PSI reactions of photosynthesis are inhibited by chilling. Seasonal chilling during winter induced photoinhibition of PSII in five of the six tropical tree species (not in *W. fruticosa*), which was evident from the significant reduction in F_v/F_m and $Y_{(II)}$ (Fig. 1, Table 1). However, the reduction of F_v/F_m during chilling was less than 20% for all species, except for *I. chinensis*, which showed a 43% reduction (Fig. 1). This suggests that photoinhibition was moderate (Huang *et al.* 2010a,b; 2016a,b). On the other hand, maximum oxidizable P700 in PSI as indicated by P_m was significantly higher across all species under chilling compared to summer. $Y_{(I)}$ was reduced in five of the six species (not in *W. fruticosa*). Regardless of species, the magnitude of changes in F_v/F_m, $Y_{(II)}$, $Y_{(I)}$, and P_m in adult trees corresponded to the response of seedlings of tropical tree species under artificially induced short-duration chilling (Elsheery *et al.* 2007, 2008; Huang *et al.* 2010a,b; 2016a,b). The higher F_v/F_m, $Y_{(II)}$, and $Y_{(I)}$ values and lower inhibition of CO_2 assimilation reaction parameters, particularly P_N and CE, of *W. fruticosa* suggest that it is the most chilling-tolerant of the tested species (Fig. 1, Table 1). Hence, responses of the light-dependent and CO_2 assimilation reactions of photosynthesis in *W. fruticosa* during chilling enabled *W. fruticosa* to cope with chilling, as discussed by comparing it with the moderate and sensitive species included in this study.

Positive correlations of F_v/F_m with P_N, g_s, and CE in both seasons (Fig. 2) revealed the strong coupling between the light-dependent and CO_2 assimilation reactions of photosynthesis. At the same time, relationships between these parameters were stronger during winter than summer. In contrast, there was no significant correlation between P_m and the above-mentioned CO_2 assimilation reaction parameters (data not shown). Furthermore, all the above positive correlations (Fig. 2) also suggest that the initial target of chilling was CO_2 assimilation reactions of photosynthesis (evident from lower P_N, g_s, and CE; Figs. 1, 2) across all species and subsequently caused moderate photoinhibition of PSII and lower electron flow (evident from lower F_v/F_m and LEF; Fig. 1). This was evident from the increased C_i and reduced g_s and the positive correlation of g_s with F_v/F_m (Fig. 2). An increase in C_i occurred at the time of slower CO_2 fixation associated with the inactivation of CO_2 assimilation reactions (as discussed above) or nonstomatal limitation. Further, higher C_i was associated with a partial closure of the stomata which suggests the simultaneous engagement of both stomatal and nonstomatal effects on P_N under chilling (Allen and Ort 2001, Raven 2014, Huang *et al.* 2016a,b; Jurczyk *et al.* 2019). Partial closure of the stomata under chilling was evident from lower g_s resulting from higher C_i.

Lower P_N and reduction of LEF between photosystems led to the moderate photoinhibition of PSII across the species and *W. fruticosa* showed the smallest reduction in LEF in winter compared to summer (Table 1). The lower rate of LEF was due to the inhibition of electron transfer from plastoquinone (PQ) to plastocyanin (PC), resulting in the increased reduction of the PQ pool. The reduced PQ pool was caused by the lower CO_2 fixation known as photosynthesis control (West and Wiskich 1968, Baker *et al.* 2007, Miyake 2020). Over-reduction of the PQ pool, which induces an inhibition of the Q-cycle in the cytochrome (Cyt) b_6/f complex and P700 oxidation is known as reduction-induced suppression of electron flow (RISE), which is also a part of photosynthesis control in cyanobacteria (Shaku *et al.* 2016, Miyake 2020). Photosynthesis control and RISE are important mechanisms to prevent deleterious photoinhibition of PSI by reducing the electron flow from PSII to PSI along with activation of alternative electron flows (CEF and WWC). Electron flow from PSII to PSI is a prerequisite for the photoinhibition of PSI and consequent secondary damages (Sonoike 2011, Miyake 2020). Because of photosynthesis control and RISE, the higher oxidation state of PSI ($P700^+$) as indicated by higher

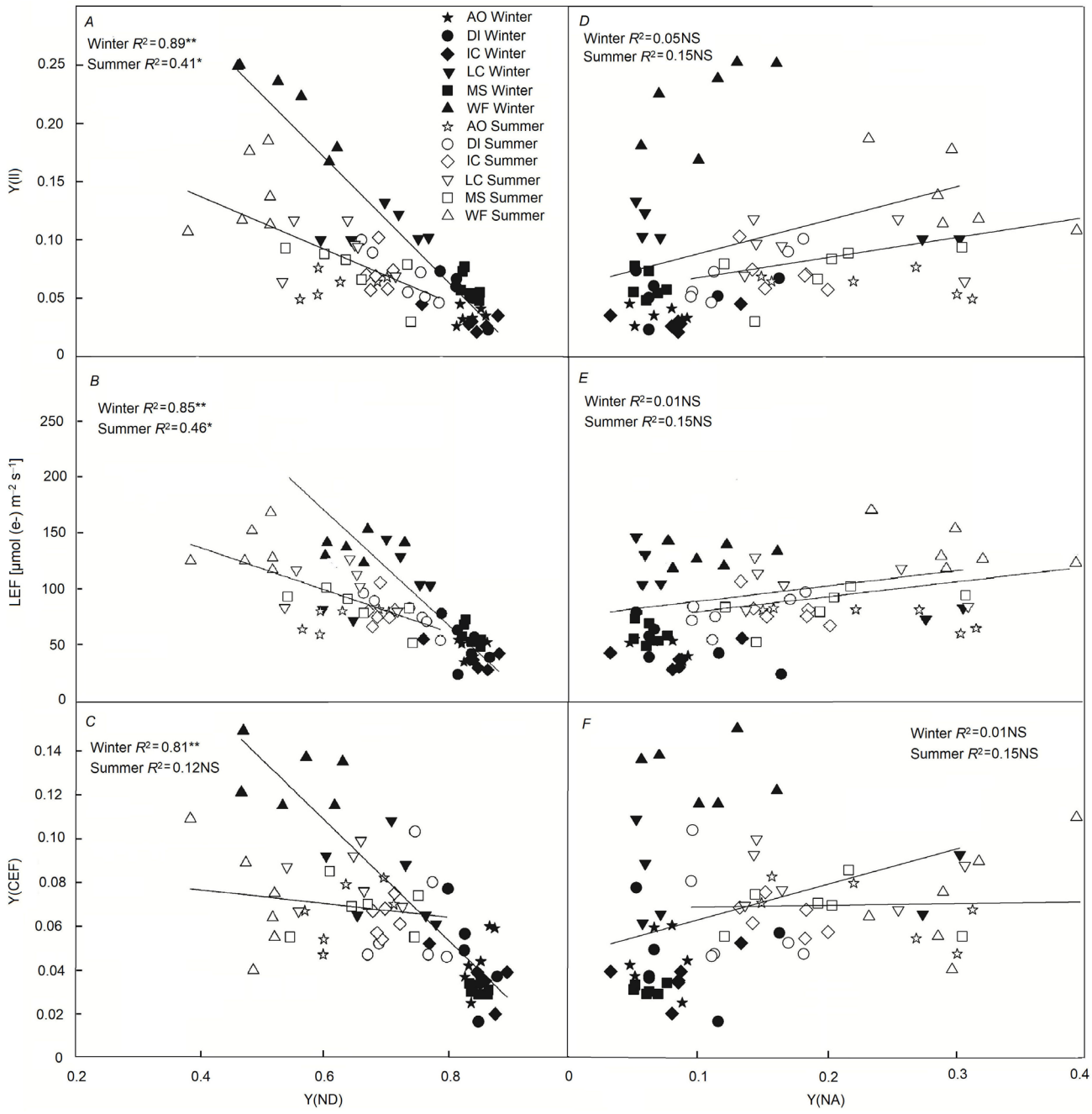

Fig. 3. Correlation of donor-side limitation of PSI [$Y_{(ND)}$] and acceptor-side limitation of PSI [$Y_{(NA)}$] with (*A*,*D*) effective photochemical quantum yield of PSII [$Y_{(II)}$], (*B*,*E*) linear electron flow (LEF), and (*C*,*F*) effective quantum yield of CEF [$Y_{(CEF)}$] during the chilling event (≤ 10°C; *closed symbols*) and summer (≥ 27°C; *open symbols*) among six tropical tree species. Coefficient of determination (R^2) followed by NS, *, and ** corresponding to non-significance, significance at P<0.05 and P<0.01, respectively. AO – *Aglaia odorata*; DI – *Dypsis lutescens*; IC – *Ixora chinensis*; LS – *Lagerstroemia speciosa*; MS – *Markhamia stipulata*; WF – *Woodfordia fruticosa*.

P_m is maintained by potential balancing of absorption and utilization of energy, and inhibition of ROS production (Miyake 2010, 2020; Sonoike 2011, Takagi *et al.* 2017, Kadota *et al.* 2019).

In this study, we assumed the existence of RISE and confirmed the photosynthesis control in all tested species with higher $Y_{(ND)}$ (Table 1), from its strong negative correlation with $Y_{(II)}$, LEF, and $Y_{(CEF)}$ under winter compared with summer (Figs. 3, 4*A*). $Y_{(ND)}$ is the electron-donor side (plastoquinone; PQ) limitation of PSI. A negative correlation of $Y_{(ND)}$ with LEF and $Y_{(II)}$ under chilling implies that the $Y_{(ND)}$ has mediated reduced electron flow between photosystems and lower efficiency of PSII to utilize light energy for photosynthesis,

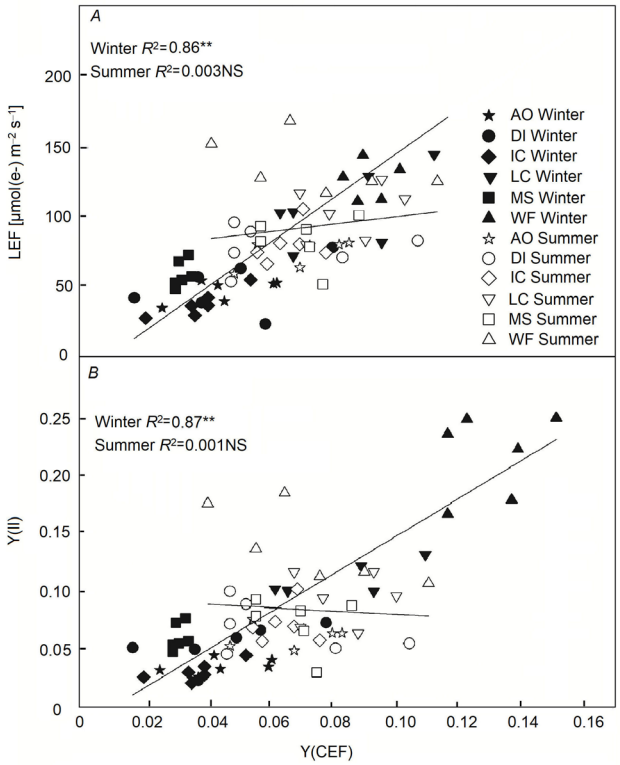

Fig. 4. Correlation of effective quantum yield of CEF [$Y_{(CEF)}$] with (*A*) linear electron flow (LEF) and (*B*) effective photochemical quantum yield of PSII [$Y_{(II)}$] during the chilling event (≤ 10°C; *closed symbols*) and summer (≥ 27°C; *open symbols*) among six tropical tree species. Coefficient of determination (R^2) followed by NS, *, and ** corresponding to non-significance, significance at P<0.05 and P<0.01, respectively. AO – *Aglaia odorata*; DI – *Dypsis lutescens*; IC – *Ixora chinensis*; LS – *Lagerstroemia speciosa*; MS – *Markhamia stipulata*; WF – *Woodfordia fruticosa*.

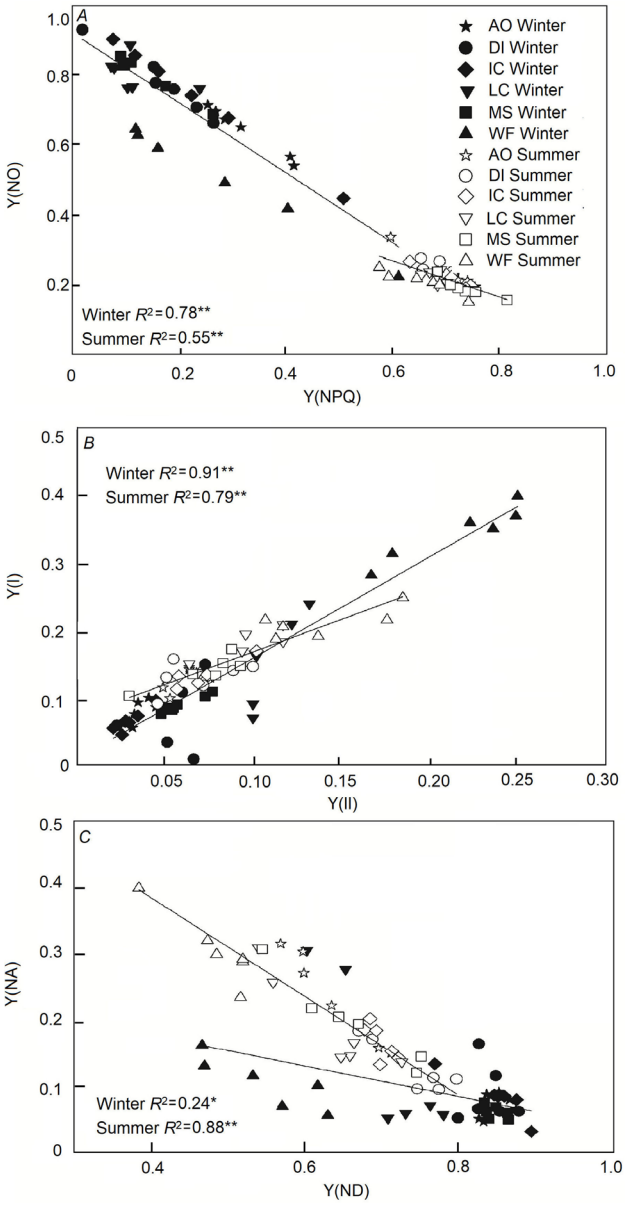

Fig. 5. Correlation between (*A*) effective quantum yield of nonphotochemical quenching [$Y_{(NPQ)}$] and yield of regulated heat dissipation of PSII [$Y_{(NO)}$], (*B*) effective photochemical quantum yield of PSII [$Y_{(II)}$] and effective photochemical quantum yield of PSI [$Y_{(I)}$], and (*C*) donor-side limitation of PSI [$Y_{(ND)}$] and acceptor-side limitation of PSI [$Y_{(NA)}$] during a chilling event (≤ 10°C; *closed symbols*) and summer (≥ 27°C; *open symbols*) among six tropical tree species. Coefficient of determination (R^2) followed by NS, *, and ** corresponding to non-significance, significance at P<0.05 and P<0.01, respectively. AO – *Aglaia odorata*; DI – *Dypsis lutescens*; IC – *Ixora chinensis*; LS – *Lagerstroemia speciosa*; MS – *Markhamia stipulata*; WF – *Woodfordia fruticosa*.

respectively. At the same time, a minor increase in $Y_{(ND)}$ was observed in the chilling-tolerant species *W. fruticosa* (Table 1). Similar trends were observed in seedlings of tropical trees exposed to chilling temperatures (Huang *et al.* 2010a,b; 2011).

A decrease in the ratio of oxidized PQ to total PQ [higher reduction of PQ (photosynthesis control and RISE) or higher $Y_{(ND)}$] supports important alternative electron flow, *i.e.*, CEF (Miyake *et al.* 2005a,b; Kubo *et al.* 2011). The correlation between $Y_{(ND)}$ and $Y_{(CEF)}$ was negative in the current study (Fig. 3*C*), which confirms the involvement of photosynthesis control and RISE in the activation or enhancement of CEF (in *W. fruticosa*), and maintenance of minimum CEF across all other species. Despite the varying degree of CEF during winter across the tree species, CEF allowed PSII to manage the electron load (Joliot and Johnson 2011) to a certain extent as evidenced by the positive correlation of $Y_{(CEF)}$ with $Y_{(II)}$ and LEF (Fig. 4).

Higher $Y_{(NA)}$ values imply that a portion of reduced electron carriers on the acceptor side of PSI could not be oxidized due to the limitation of CO_2 assimilation reactions, particularly caused by lower P_N and higher C_i (Shimakawa and Miyake 2018, Miyake 2020). While in this study, similar to the response of seedlings of tropical tree species observed in earlier studies by Huang *et al.*

(2010a,b; 2011), $Y_{(NA)}$ was lower during winter than in summer (Table 1). This contradiction in $Y_{(NA)}$ under chilling across species with lower P_N and higher C_i can be attributed to lower F_v/F_m, higher $Y_{(ND)}$, and CEF, which supported the oxidative status of P700 in PSI ($P700^+$). In contrast to $Y_{(ND)}$, there was no correlation between $Y_{(NA)}$ and any of the other measured physiological parameters in both seasons, except P_m (Fig. 3).

A weak negative correlation between $Y_{(ND)}$ and LEF, $Y_{(CEF)}$ and $Y_{(II)}$ during summer, compared to winter, was due to the favorable weather conditions, which enabled faster photosynthesis, thus leading to unclogged electron flow between photosystems (Figs. 1*B*, 3; Table 1). On the other hand, lower $Y_{(ND)}$ and P_m and higher $Y_{(NA)}$ and CEF in four of the six species during summer (Table 1) can be attributed to the high ambient light intensity as PSI is susceptible to high light intensity in summer or due to the acclimation and higher PSII to PSI ratio (Fig. 1S) (Barth and Krause 1999, Miyake *et al.* 2004, 2005a,b; Kubo *et al.* 2011, Kono and Terashima 2016).

CEF may be negligible in favorable growth conditions (Kou *et al.* 2013, Kadota *et al.* 2019), under chilling greater significance of CEF was evident from the response of tolerant *W. fruticosa* compared with the other four moderately tolerant species, whereas no significant change in CEF was observed in the *L. speciosa* (Table 1). This is consistent with the previous finding of activation of CEF with increased photoinhibition and limited photosynthesis (Miyake *et al.* 2004, 2005a,b; Takahashi *et al.* 2009, Agrawal *et al.* 2016, Neto *et al.* 2017). There are several main functions of CEF involved in the mitigation of the impact of stress, thereby preventing severe damage to PSII and ultimately PSI: (*1*) to synthesize ATP to support LEF and to maintain the balance of ATP and NADPH consumption; (*2*) to generate a higher proton gradient (ΔpH) along with LEF for the activation of NPQ to protect PSII thereby maintaining electron flow; (*3*) to protect the oxygen-evolving complex (OEC) inside the thylakoid lumen, which is the primary site for photodamage in PSII and *de novo* synthesis of D1 protein; (*4*) to maintain the balance of $Y_{(ND)}$ and $Y_{(NA)}$ to protect PSI from photoinhibition; and (*5*) to limit ROS production at PSII and PSI (Müller *et al.* 2001, Mohanty *et al.* 2007, Miyake 2010, 2020; Allakhverdiev 2011, Joliot and Johnson 2011, Sonoike 2011, Kono and Terashima 2016, Huang *et al.* 2018, Kadota *et al.* 2019).

The reduced $Y_{(NPQ)}$ and its significant negative correlation with $Y_{(NO)}$ across species under chilling indicates a lower level of stimulation of NPQ during photoinhibition of PSII, and thereby an intensified inhibition of the chain of reactions of photosynthesis (Table 1, Fig. 5*A*), which was similar to the trend in seedlings of tropical trees exposed to chilling temperatures (Huang *et al.* 2010a,b; 2011). The higher $Y_{(NO)}$ indicates that both photochemical energy conversion and protective regulatory mechanisms were not effective in preventing the photoinhibition of PSII. Low values of $Y_{(NPQ)}$ under chilling across the six species indicate lower regulated photoprotective activity through the xanthophyll cycle. Such a state of NPQ can take place when the ΔpH between thylakoid lumen and stroma is inadequate due to reduced LEF and inactive or insufficient CEF for the conformational change of PsbS protein structure, which acts as a ΔpH sensor to activate NPQ (Joliot and Joliot 2006, Miyake 2010, Yamori and Shikanai 2016, Zheng *et al.* 2019). However, low $Y_{(NO)}$ and high $Y_{(NPQ)}$ values in *W. fruticosa* compared with the other species (except *A. odorata* which showed higher $Y_{(NPQ)}$ than *W. fruticosa*) further confirms the importance of CEF for chilling tolerance. Conversely, *L. speciosa* showed higher CEF next to *W. fruticosa*, but lower $Y_{(NPQ)}$, F_v/F_m, P_N, CE, and $Y_{(II)}$ and higher $Y_{(NO)}$ and $Y_{(I)}$ under chilling across all species (Table 1). Interestingly, stimulation of CEF should trigger an NPQ-mediated ΔpH with assistance from PsbS protein, which was not observed in *L. speciosa*. This can be due to the inadequacy of the ΔpH created by the stimulation of CEF in *L. speciosa* to increase NPQ. Alternatively, it may be due to the conformational changes in PsbS protein structure that led to a lower degree of NPQ, thereby resulting in higher photoinhibition of PSII. Meanwhile, *A. odorata* showed an opposite trend to *L. speciosa* (Table 1). This species showed lower CEF, but higher $Y_{(NPQ)}$ than *W. fruticosa*, with lower F_v/F_m, P_N, CE, $Y_{(II)}$, and $Y_{(I)}$ and higher $Y_{(NO)}$. This might be explained by the higher level of structural damage in PSII in *A. odorata* which impaired efficient management of excess energy even after a higher activation of NPQ. Further studies are required to clarify these controversial results and to understand the mechanisms underlying photodamage.

In summary, a seasonal chilling event induced moderate photoinhibition of PSII in the majority of the tested tropical tree species. Stomatal and nonstomatal regulations on photosynthesis under chilling resulted in reduced fixation and light-dependent reactions, such as a slower rate of LEF by increasing photosynthesis control and thereby higher oxidation state of PSI that prevented photoinhibition of PSI. *Woodfordia fruticosa* was the least affected by chilling as demonstrated by a lower reduction of photosynthetic rate and photochemical efficiency of PSII and higher CEF and oxidation state of P700 in PSI compared with the other species. Correlation analysis suggested that the light-dependent and CO_2 assimilation reactions of photosynthesis were closely coupled across all tree species in each season, with stronger coupling in winter. The tropical tree species demonstrated a range of strategies to regulate photosynthesis by rearranging the degree of photoprotection mechanisms according to seasonal meteorological conditions. The present results have implications for screening tropical plant species to improve planning for the management of urban landscapes based on future climatic predictions.

References

Agrawal D., Allakhverdiev S.I., Jajoo A.: Cyclic electron flow plays an important role in protection of spinach leaves under high temperature stress. – Russ. J. Plant Physiol. **63**: 210-215, 2016.

Allakhverdiev S.I.: Recent progress in the studies of structure and function of photosystem II. – J. Photoch. Photobio. B **104**: 1-8, 2011.

Allen D.J., Ort D.R.: Impacts of chilling temperatures on photosynthesis in warm-climate plants. – Trends Plant Sci. **6**: 36-42, 2001.

Allen D.J., Ratner K., Giller Y.E. *et al.*: An overnight chill induces a delayed inhibition of photosynthesis at midday in mango (*Mangifera indica* L.). – J. Exp. Bot. **51**: 1893-902, 2000.

Asada K.: Production and scavenging of reactive oxygen species in chloroplasts and their functions. – Plant Physiol. **141**: 391-396, 2006.

Baker N.R., Harbinson J., Kramer D.M.: Determining the limitations and regulation of photosynthetic energy transduction in leaves. – Plant Cell Environ. **30**: 1107-1125, 2007.

Barth C., Krause G.H.: Inhibition of photosystems I and II in chilling-sensitive and chilling-tolerant plants under light and low-temperature stress. – Z. Naturforsch. **54c**: 645-657, 1999.

Belgio E., Kapitonova E., Chmeliov J. *et al.*: Economic photoprotection in photosystem II that retains a complete light-harvesting system with slow energy traps. – Nat. Commun. **5**: 4433, 2014.

Bukhov N.G., Carpentier R.: Heterogeneity of photosystem II reaction centers as influenced by heat treatment of barley leaves. – Physiol. Plantarum **110**: 279-285, 2000.

Derks A., Schaven K., Bruce D.: Diverse mechanisms for photoprotection in photosynthesis. Dynamic regulation of photosystem II excitation in response to rapid environmental change. – BBA-Bioenergetics **1847**: 468-485, 2015.

Elsheery N.I., Sunoj V.S.J., Wen Y. *et al.*: Foliar application of nanoparticles mitigates the chilling effect on photosynthesis and photoprotection in sugarcane. – Plant Physiol. Bioch. **149**: 50-60, 2020.

Elsheery N.I., Wilske B., Cao K.F.: The effect of night chilling on gas exchange and chlorophyll fluorescence of two mango cultivars growing under two irradiances. – Acta Bot. Yunnan. **30**: 447-456, 2008.

Elsheery N.I., Wilske B., Zhang J.L., Cao K.F.: Seasonal variations in gas exchange and chlorophyll fluorescence in the leaves of five mango cultivars in southern Yunnan, China. – J. Hortic. Sci. Biotech. **82**: 855-862, 2007.

Foyer C.H., Shigeoka S.: Understanding oxidative stress and antioxidant functions to enhance photosynthesis. – Plant Physiol. **155**: 93-100, 2011.

Gao S., Wang G.: The enhancement of cyclic electron flow around photosystem I improves the recovery of severely desiccated *Porphyra yezoensis* (Bangiales, Rhodophyta). – J. Exp. Bot. **12**: 4349-4358, 2012.

Genty B., Briantais J.M., Baker N.R.: The relationship between the quantum yield of photosynthetic electron transport and quenching of chlorophyll fluorescence. – BBA-Gen. Subjects **990**: 87-92, 1989.

Gratani L., Catoni R., Varone L.: Morphological, anatomical and physiological leaf traits of *Q. ilex*, *P. latifolia*, *P. lentiscus*, and *M. communis* and their response to Mediterranean climate stress factors. – Bot. Stud. **54**: 35, 2013.

Guidi L., Lo Piccolo E., Landi M.: Chlorophyll fluorescence, photoinhibition and abiotic stress: Does it make any difference the fact to be a C_3 or C_4 species? – Front. Plant Sci. **10**: 174, 2019.

Huang W., Hu H., Zhang S.: Photosynthesis and photosynthetic electron flow in the alpine evergreen species *Quercus guyavifolia* in winter. – Front. Plant Sci. **7**: 1511, 2016b.

Huang W., Quan X., Zhang S.B., Liu T.: *In vivo* regulation of proton motive force during photosynthetic induction. – Environ. Exp. Bot. **148**: 109-116, 2018.

Huang W., Yang Y.J., Hu H. *et al.*: Sustained diurnal stimulation of cyclic electron flow in two tropical tree species *Erythrophleum guineense* and *Khaya ivorensis*. – Front. Plant Sci. **7**: 1068, 2016a.

Huang W., Zhang S.B., Cao K.F.: Stimulation of cyclic electron flow during recovery after chilling-induced photoinhibition of PSII. – Plant Cell Physiol. **51**: 1922-1928, 2010a.

Huang W., Zhang S.B., Cao K.F.: The different effects of chilling stress under moderate light intensity on photosystem II compared with photosystem I and subsequent recovery in tropical tree species. – Photosynth. Res. **103**: 175-182, 2010b.

Huang W., Zhang S.B., Cao K.F.: Cyclic electron flow plays an important role in photoprotection of tropical trees illuminated at temporal chilling temperature. – Plant Cell Physiol. **52**: 297-305, 2011.

Huang W., Zhang S.B., Xu J.C., Liu T.: Plasticity in roles of cyclic electron flow around photosystem I at contrasting temperatures in the chilling-sensitive plant *Calotropis gigantea*. – Environ. Exp. Bot. **141**: 145-153, 2017.

Huang W., Zhang S.B., Zhang J.L., Hu H.: Photoinhibition of photosystem I under high light in the shade-established tropical tree species *Psychotria rubra*. – Front. Plant Sci. **6**: 801, 2015.

Jalili A., Jamzad Z., Thompson K. *et al.*: Climate change, unpredictable cold waves and possible brakes on plant migration. – Global Ecol. Biogeogr. **19**: 642-648, 2010.

Joliot P., Johnson G.N.: Regulation of cyclic and linear electron flow in higher plants. – P. Natl. Acad. Sci. USA **108**: 13317-13322, 2011.

Joliot P., Joliot A.: Cyclic electron flow in C_3 plants. – BBA-Bioenergetics **1757**: 362-368, 2006.

Jurczyk B., Grzesiak M., Pociecha E. *et al.*: Diverse stomatal behaviors mediating photosynthetic acclimation to low temperatures in *Hordeum vulgare*. – Front. Plant Sci. **9**: 1963, 2019.

Kadota K., Furutani R., Makino A. *et al.*: Oxidation of P700 induces alternative electron flow in photosystem I in wheat leaves. – Plants-Basel **8**: 152, 2019.

Khatoon M., Inagawa K., Pospíšil P. *et al.*: Quality control of photosystem II: Thylakoid unstacking is necessary to avoid further damage to the D1 protein and to facilitate D1 degradation under light stress in spinach thylakoids. – J. Biol. Chem. **284**: 25343-25352, 2009.

Klughammer C., Schreiber U.: An improved method, using saturating light pulses, for the determination of photosystem-I quantum yield via $P700^+$ absorbance changes at 830 nm. – Planta **192**: 261-268, 1994.

Klughammer C., Schreiber U.: Complementary PSII quantum yields calculated from simple fluorescence parameters measured by PAM fluorometry and the Saturation Pulse method. – PAM Appl. Notes **1**: 27-35, 2008.

Kono M., Terashima I.: Elucidation of photoprotective mechanisms of PSI against fluctuating light photoinhibition. – Plant Cell Physiol. **57**: 1405-1414, 2016.

Körner C.: Plant adaptation to cold climates. – F1000Research **5**: 2769, 2016.

Kou J., Takahashi S., Oguchi R. *et al.*: Estimation of the steady-state cyclic electron flux around PSI in spinach leaf discs in white light, CO_2-enriched air and other varied conditions. – Funct. Plant Biol. 4: 1018-1028, 2013.

Kramer D.M., Johnson G., Kiirats O., Edwards G.E.: New fluorescence parameters for the determination of Q_A redox state and excitation energy fluxes. – Photosynth. Res. **79**: 209-218, 2004.

Kubo S., Masumura T., Saito Y. *et al.*: Cyclic electron flow

around PSI functions in the photoinhibited rice leaves. – Soil Sci. Plant Nutr. **57**: 105-113, 2011.

Li Y., Liu J., Zhou G. *et al.*: Warming effects on photosynthesis of subtropical tree species: a translocation experiment along an altitudinal gradient. – Sci. Rep.-UK **6**: 24895, 2016.

Li Y., Sunoj V.S.J., Short A.W. *et al.*: Correlations between allocation to foliar phosphorus fractions and maintenance of photosynthetic integrity in six mangrove populations as affected by chilling. – New Phytol. **232**: 2267-2282, 2021.

Liu X., Zhou Y., Xiao J., Bao F.: Effects of chilling on the structure, function and development of chloroplasts. – Front Plant Sci. **9**: 1715, 2018.

Mathur S., Sunoj V.S.J., Elsheery N.I. *et al.*: Regulation of photosystem II heterogeneity and photochemistry in two cultivars of C_4 crop sugarcane under chilling stress. – Front. Plant Sci. **12**: 627012, 2021.

Mau A.C., Reed S.C., Wood T.E., Cavaleri M.A.: Temperate and tropical forest canopies are already functioning beyond their thermal thresholds for photosynthesis. – Forests **9**: 47, 2018.

Maxwell K., Johnson G.N.: Chlorophyll fluorescence – a practical guide. – J. Exp. Bot. **51**: 659-668, 2000.

Miyake C.: Alternative electron flows (water–water cycle and cyclic electron flow around PSI) in photosynthesis: Molecular mechanisms and physiological functions. – Plant Cell Physiol. **51**: 1951-1963, 2010.

Miyake C.: Molecular mechanism of oxidation of P700 and suppression of ROS production in photosystem I in response to electron-sink limitations in C_3 plants. – Antioxidants **9**: 230, 2020.

Miyake C., Horiguchi S., Makino A. *et al.*: Effects of light intensity on cyclic electron flow around PSI and its relationship to non-photochemical quenching of Chl fluorescence in tobacco leaves. – Plant Cell Physiol. **l46**: 1819-1830, 2005b.

Miyake C., Miyata M., Shinzaki Y., Tomizawa K.: CO_2 response of cyclic electron flow around PSI (CEF-PSI) in tobacco leaves: Relative electron fluxes through PSI and PSII determine the magnitude of non-photochemical quenching (NPQ) of Chl fluorescence. – Plant Cell Physiol. **46**: 629-637, 2005a.

Miyake C., Shinzaki Y., Miyata M., Tomizawa K.: Enhancement of cyclic electron flow around PSI at high light and its contribution to the induction of non-photochemical quenching of Chl fluorescence in intact leaves of tobacco plants. – Plant Cell Physiol. **45**: 1426-1433, 2004.

Mohanty P., Allakhverdiev S.I., Murata N.: Application of low temperatures during photoinhibition allows characterization of individual steps in photodamage and the repair of photosystem II. – Photosynth. Res. **94**: 217-224, 2007.

Müller P., Li X.-P., Niyogi K.K.: Non-photochemical quenching. A response to excess light energy. – Plant Physiol. **125**: 1558-1566, 2001.

Murata N., Allakhverdiev S.I., Nishiyama Y.: The mechanism of photoinhibition *in vivo*: Re-evaluation of the roles of catalase, α-tocopherol, non-photochemical quenching, and electron transport. – BBA-Bioenergetics **1817**: 1127-1133, 2012.

Murata N., Takahashi S., Nishiyama Y., Allakhverdiev S.I.: Photoinhibition of photosystem II under environmental stress. – BBA-Bioenergetics **1767**: 414-421, 2007.

Murchie E.H., Niyogi K.K.: Manipulation of photoprotection to improve plant photosynthesis. – Plant Physiol. **155**: 86-92, 2011.

Neto M.C.L., Cerqueira J.V.A., da Cunha J.R. *et al.*: Cyclic electron flow, NPQ and photorespiration are crucial for the establishment of young plants of *Ricinus communis* and *Jatropha curcas* exposed to drought. – Plant Biol. **19**: 650-659, 2017.

Oxborough K., Baker N.R.: Resolving chlorophyll *a* fluorescence images of photosynthetic efficiency into photochemical and non-photochemical components – calculation of q_P and F_v'/F_m' without measuring F_o'. – Photosynth. Res. **54**: 135-142, 1997.

Raven J.A.: Speedy small stomata? – J. Exp. Bot. **65**: 1415-1424, 2014.

Rutherford A.W., Krieger-Liszkay A.: Herbicide-induced oxidative stress in photosystem II. – Trends Biochem. Sci. **26**: 648-653, 2001.

Rymbai H., Laxman R.H., Dinesh M.R. *et al.*: Diversity in leaf morphology and physiological characteristics among mango (*Mangifera indica*) cultivars popular in different agro-climatic regions of India. – Sci. Hortic.-Amsterdam **176**: 189-193, 2014.

Shaku K., Shimakawa G., Hashiguchi M., Miyake C.: Reduction-induced suppression of electron flow (RISE) in the photosynthetic electron transport system of *Synechococcus elongatus* PCC 7942. – Plant Cell Physiol. **57**: 1443-1453, 2016.

Shimakawa G., Miyake C.: Oxidation of P700 ensures robust photosynthesis. – Front. Plant. Sci. **9**: 1617, 2018.

Someralo S., Krause G.H.: Photoinhibition at chilling temperatures and effects of freezing stress on cold acclimated spinach leaves in the field. A fluorescence study. – Physiol. Plantarum **79**: 617-622, 1990.

Sonoike K.: Degradation of *psa B* gene product, the reaction center subunit of photosystem I, is caused during photoinhibition of photosystem I: possible involvement of active oxygen species. – Plant Sci. **115**: 157-164, 1996.

Sonoike K.: Photoinhibition of photosystem I. – Physiol. Plantarum **142**: 56-64, 2011.

Takagi D., Ishizaki K., Hanawa H. *et al.*: Diversity of strategies for escaping reactive oxygen species production within photosystem I among land plants: P700 oxidation system is prerequisite for alleviating photoinhibition in photosystem I. – Physiol. Plantarum **161**: 56-74, 2017.

Takahashi S., Milward S.E., Fan D.Y. *et al.*: How does cyclic electron flow alleviate photoinhibition in *Arabidopsis*? – Plant Physiol. **149**: 1560-1567, 2009.

Tikkanen M., Mekala N.R., Aro E.M.: Photosystem II photoinhibition-repair cycle protects Photosystem I from irreversible damage. – BBA-Bioenergetics **1837**: 210-215, 2014.

Wen Y., Qin D.W., Leng B. *et al.*: The physiological cold tolerance of warm-climate plants is correlated with their latitudinal range limit. – Biol. Lett. **14**: 20180277, 2018.

West K.R., Wiskich J.T.: Photosynthetic control by isolated pea chloroplasts. – Biochem. J. **109**: 527-532, 1968.

Wu J., Nadeem M., Galagedara L. *et al.*: Effects of chilling stress on morphological, physiological, and biochemical attributes of silage corn genotypes during seedling establishment. – Plants-Basel **11**: 1217, 2022.

Yamori W., Shikanai T.: Physiological functions of cyclic electron transport around photosystem I in sustaining photosynthesis and plant growth. – Annu. Rev. Plant Biol. **67**: 81-106, 2016.

Yang Y.J., Chang W., Huang W. *et al.*: The effects of chilling-light stress on photosystems I and II in three *Paphiopedilum* species. – Bot. Stud. **58**: 53, 2017.

Zhang S., Scheller H.V.: Photoinhibition of photosystem I at chilling temperature and subsequent recovery in *Arabidopsis thaliana*. – Plant Cell Physiol. **45**: 1595-1602, 2004.

Zheng C., Tang J., Chen J. *et al.*: Mechanisms on inhibition of photosynthesis in *Kandelia obovata* due to extreme cold events under climate change. – Ecol. Process. **5**: 20, 2016.

Zheng X.-T., Chen Y.-L., Zhang X.-H. *et al.*: ANS-deficient *Arabidopsis* is sensitive to high light due to impaired anthocyanin photoprotection. – Funct. Plant Biol. **46**: 756-765, 2019.

Zivcak M., Brestic M., Kunderlikova K. *et al.*: Repetitive light pulse-induced photoinhibition of photosystem I severely affects CO_2 assimilation and photoprotection in wheat leaves. – Photosynth. Res. **126**: 449-463, 2015.

© The authors. This is an open access article distributed under the terms of the Creative Commons BY-NC-ND Licence.